

UWB Radar Imaging of Multiple Targets through Multi-Layer Walls

Huamei Zhang* Yerong Zhang and Fangfang Wang

School of Electronic Science and Engineering, Nanjing University of Posts and Telecommunications, Nanjing 210003, China
zhanghm@njupt.edu.cn

Abstract

In the practical application of Ultra Wideband (UWB) through-wall radar imaging, the walls that are generally encountered consist of multiple layers, and there may be multiple targets, which presents challenges for the imaging algorithm. In this study, both the back-projection (BP) algorithm, which is a time-domain algorithm, and the phase-shift migration (PSM) algorithm, which is a frequency-domain algorithm, are used to locate two targets behind a two-layer wall. The image quality, the azimuth and range resolutions, the image entropy and the processing time of the two algorithms are compared. The simulation results demonstrate that the BP algorithm produces better image quality and that the PSM algorithm is faster. The effect of the sampling interval on the image entropy and processing time is discussed. In addition, the feasibility and the validity of the two algorithms are tested under noisy conditions. The results show that the two algorithms are robust, regardless of the presence of noise.

Keywords: *through-wall radar, imaging, back-projection algorithm, phase-shift migration algorithm*

1. Introduction

Through-wall radar imaging (TWRI) is a form of nondestructive detection that can sense through obstacles such as walls, doors, and other visually opaque materials. TWRI has played an important role in fighting terrorism, natural disaster relief, surveillance and reconnaissance in urban environments and other search activities and thus has become more attractive in many civilian and military applications [1,2].

In TWRI, accurately representing the propagation of the electromagnetic waves in building walls is crucial for the image quality [3]. For simplicity, various studies have assumed a single layer and a homogeneous model of the building wall[4,5], and focused, high-quality images were obtained through accurate compensation[6,7]. In practice, however, walls have multiple layers and are inhomogeneous, and there may be multiple targets behind a wall, additional problems that must be considered.

Usually, imaging algorithms process data in either the time or frequency domain. The BP algorithm is a conventional delay-and-sum beamforming algorithm that belongs to the time-domain category and is the most commonly used imaging algorithm in TWRI [4,8]. The BP algorithm is simple and easy to understand, but the computational efficiency is low in the presence of walls. Because the propagation path of the electromagnetic waves changes at every interface between materials of different types, the refraction point must be accurately located. Otherwise, the resulting image is not focused and displaced from the true target

* Corresponding Author

position. If the wall has multiple layers, the computational time grows exponentially. The PSM algorithm is based on the wave equation and belongs to the frequency-domain category of imaging algorithms. This algorithm was first proposed by Gazdag in 1978[9] for wavenumber migration and can be used iteratively to refocus seismic or radar images. The PSM algorithm reconstructs images using the fast Fourier transform (FFT), which avoids the time-consuming ray-tracing process and is significantly faster than other methods. More importantly, the PSM algorithm allows the wave velocity to vary with depth and has been successfully applied in synthetic aperture focusing in multilayered media[10,11]. The general scenario of TWRI involves layered structures, so the PSM algorithm is also suitable for TWRI [12]. If the thickness and the electromagnetic parameters of a wall are known, then real-time, high-quality images can be obtained with the PSM algorithm.

In this study, a two-layer wall model is developed, and simulations are conducted using a time-domain finite difference (FDTD) method. The BP algorithm and the PSM algorithm are used to locate two targets behind a wall, and the results obtained from the two algorithms are compared. The paper is organized as follows. In Section 2, we present the FDTD model, the BP algorithm, the PSM algorithm and the entropy criterion. The experimental results are given and compared in Section 3. Section 4 provides concluding remarks.

2. Formulations

2.1. FDTD Model

Figure 1 shows the general scenario of TWRI with two targets behind a two-layer wall. The origin of the coordinate system is located at the top left corner of the upper layer. The thicknesses of the upper and lower layers are $d_u=0.1\text{ m}$ and $d_l=0.05\text{ m}$, respectively, and for the relative permittivity of the upper and lower layers, standard values of $\epsilon_{ru}=4.5$ and $\epsilon_{rl}=2.6$, respectively, were used. The imaging area behind a two-layer wall is free space with dielectric permittivity and magnetic permeability denoted by ϵ_0 and μ_0 . Its length is 2.4 m and its width is 2.6 m. Two square metal bodies whose length is 0.11m reside in the imaging area, and the center coordinate of them are (0.65 m, 0.65 m), (1.65 m, 1.45 m).

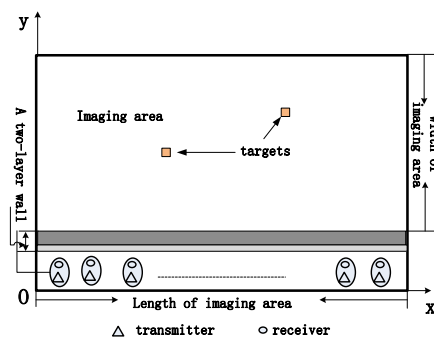


Figure 1. General Scenario of TWRI Problem

The data is generated by the 2D FDTD method. The geometry of the TWRI is discretized with the FDTD square cells of 1cm length. The time resolutions is 16.7 ps. The antenna which transmit and receive signals moves parallel to the wall and synthesizes a measurement aperture $L=2.4\text{ m}$. The excited source is chosen as the

sinusoidal modulated Gaussian pulse at center frequency 2 GHz with 2.1 GHz bandwidth.

The imaging data are collected from the receiving antenna array. In forward modeling, a set of electric field values as functions of the time traveled by the radar signals is obtained. Scattered echo data were obtained using the background subtraction method, which subtracts electric field values with and without targets.

2.2. BP Algorithm

The BP algorithm originates from computer tomography and is characterized by a time delay, which eliminates the effect of the Doppler shift and greatly simplifies the calculations. The scattered data were processed with the BP algorithm, which was implemented as follows:

Step 1. Divide the whole region of interest into small surface areas or pixels.

Step 2. For each pixel, calculate the total flight time from transmitter to pixel and pixel to a receiver.

Step 3. Record the corresponding received time bin amplitude for each pixel.

Step 4. Repeat step 2 and 3 for all receivers.

Step 5. Sum the recorded amplitudes on the spatial grid.

In free space, the back projected signal at pixel (x, y) is given by:

$$I(x, y) = \sum_n E(t(n)) \quad (1)$$

where $t(n) = t_{xyt} + t_{xyr}$ is the total time for the transmitted signal to travel to pixel and then travel back to receiver n ; c is the speed of light in free space; t_{xyt} is the propagation time between the transmitter antenna and pixel; and t_{xyr} is the propagation time between pixel and the receiver antenna. $E(t(n))$ is the sum of the signal amplitudes.

When an electromagnetic wave encounters a wall, the path of the wave changes. If the refraction points can be accurately determined, then the transmission path and the reflection coefficient can be determined. The precise refraction point can be found using quadratic equations. When the wall consists of two or more layers, an analytical solution exists, but the equations are exceedingly complicated, thus making calculations impractical. According to Fermat's principle, the propagation time is shortest if the electromagnetic waves travel along the actual path. In this study, a search method that finds the shortest time is used to find the refraction points at the various interfaces. Then, t_{xyt} is calculated accurately.

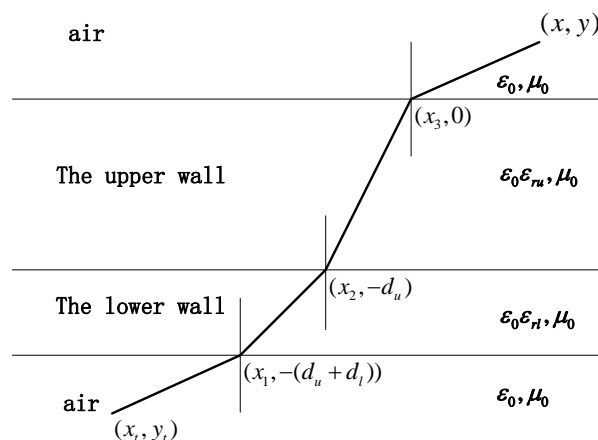


Figure 2. Geometry Depicting the Effect of Refraction on Propagation

Figure 2 shows the geometry of the electromagnetic propagation through a two-layer wall. We assume that the transmitter antenna with coordinate (x_t, y_t) is located in air before the wall and that a point target with coordinate (x, y) is located in air behind the wall. When the electromagnetic wave transmits through the wall, refraction will happen at the interface between the wall and the air. the refraction point is $(x_1, -(d_u + d_l))$, which is at the interface between air and the lower wall, $(x_2, -d_u)$, which is at the interface between the lower wall and the upper wall, and $(x_3, 0)$, which is at the interface between the upper wall and the air.

The transmission time of electromagnetic waves from the transmitter antenna to the pixel is calculated as follows:

Propagation distance of the signal inside the lower wall: $l_1 = \sqrt{(x_1 - x_2)^2 + d_l^2}$.

Propagation distance of the signal inside the upper wall: $l_2 = \sqrt{(x_2 - x_3)^2 + d_u^2}$.

Propagation distance of the signal inside the free space: $l_3 = \sqrt{(x - x_3)^2 + y^2}$,
 $l_4 = \sqrt{(x_t - x_1)^2 + (y_t + d_l + d_u)^2}$.

The total time for the signal to travel from the transmitter antenna to the pixel is:

$$t_{xyt}(n) = \frac{\sqrt{\epsilon_{rl}}l_1 + \sqrt{\epsilon_{ru}}l_2 + l_3 + l_4}{c} \quad (2)$$

Using the same method, t_{xyr} is also obtained.

So the imaging function is:

$$I(x, y) = \sum_n E(t_{xyt} + t_{xyr}) \quad (3)$$

Thus, the time delay is well compensated.

2.3. PSM Algorithm

The PSM algorithm is a frequency-wavenumber algorithm. The basic principle is that the received signal is inversely extrapolated in the frequency domain and the wave field at every depth for $t=0$ is reconstructed using the inverse FFT(IFFT). The wave field can then be computed to an arbitrary depth.

We assume the abscissa of the receiver antenna is x , the ordinate is y_0 , and the scatter signal is $e(x, y_0, t)$, the procedure of 2D PSM algorithm is as following.

Step 1. Fourier transform the data over x and t .

$$E(k_x, y_0, \omega) = \iint e(x, y_0, t) \exp(-jk_x x) \exp(-j\omega t) dx dt \quad (4)$$

Step 2. the wave field is recursively extrapolated in frequency-wavenumber domain and the continuation step size is Δy . If Δy is smaller than the thickness of every-layer medium, longitudinal velocity v is unchanged inside each Δy interval. For transmit antennas works as receive antenna at the same time, a constant offset during data acquisition is considered, and the wave field at a new depth $y_1 = y_0 + \Delta y$ is computed as follows:

$$E(k_x, y_1, \omega) = E(k_x, y_0, \omega) \exp(j\sqrt{\frac{4\omega^2}{v^2} - k_x^2} \Delta y) \quad (5)$$

Step 3. Inverse Fourier transform the wavenumber data over k_x and ω , and set $t=0$,

$$e(x, y_1, t=0) = \frac{1}{4\pi^2} \int E(k_x, y_1, \omega) \exp(jk_x x) dk_x d\omega \quad (6)$$

Where $e(x, y_1, t=0)$ is the result of phase-shift operation at the depth $y = y_1$.

Step 4. Repeat steps 2 and 3 for every depth $y_{m+1} = y_m + \Delta y$, where $m=0,1,\dots,M-1$.

2.4. Entropy Criterion

The imaging quality is determined by the minimum entropy criterion. To compare the BP algorithm and the PSM algorithm, the entropy of the image is defined as in (7):

$$\xi = \left(\sum \sum |x_{ij}|^2 \right)^2 / \sum \sum |x_{ij}|^4 \quad (7)$$

where $|x_{ij}|$ denotes the field amplitude of the (i, j) th FDTD cell. The smaller the value of the entropy criterion is, the better the quality.

3. Experimental Results

In this section, the BP and PSM algorithms are used to obtain images of targets and the results are compared.

The BP and PSM imaging results are given in Figures. 3 and 4, respectively, where subfigures (a), (b), and (c) show the 2D image, the azimuth-normalized amplitude distribution map, and the range-normalized amplitude distribution map, respectively.

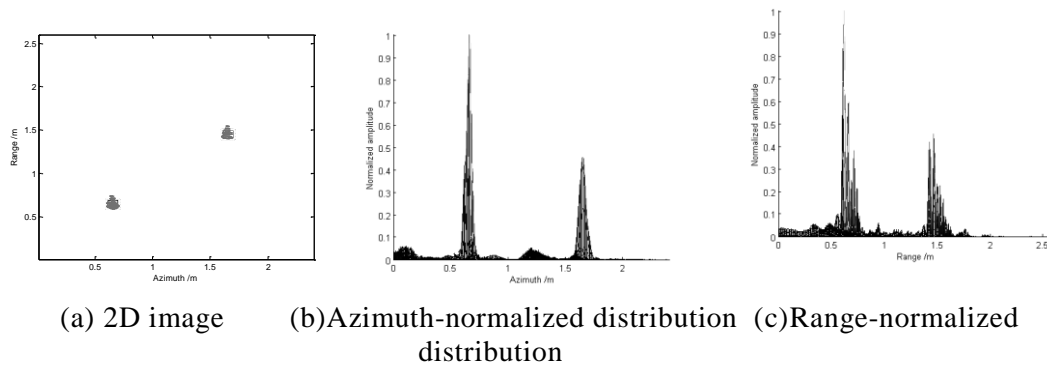


Figure 3. BP Imaging Results

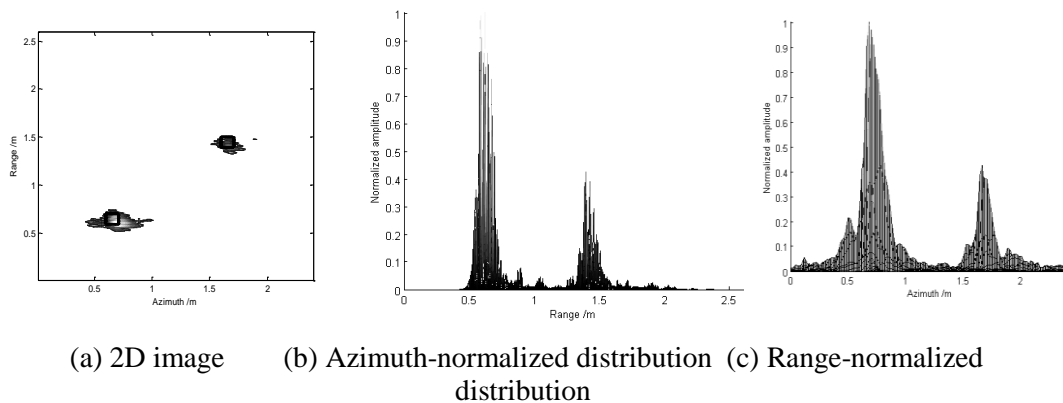
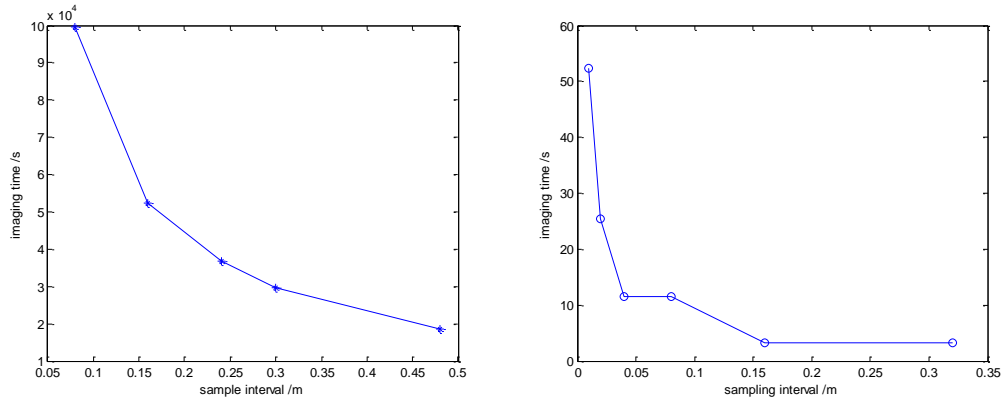


Figure 4. PSM Imaging Results

From Figures. 3 and 4, we observe that both algorithms are suitable for Ultra Wideband (UWB) radar imaging of multiple targets through multi-layer walls and can locate the targets precisely. The azimuthal resolution of the BP algorithm is higher than that of the PSM algorithm, whereas the range resolution of the two algorithms is nearly equal.

Figure 5 shows the dependence of the processing time on the sampling interval size, where 5(a) is for the BP algorithm and 5(b) is for the PSM algorithm. The

processing time decreases as the sampling interval increases for both algorithms. For both algorithms, the processing time remains on the same order, regardless of the sampling interval size: for the BP algorithm, the computation time is on the order of tens of thousands of seconds, and for the PSM algorithm, the computation time is on the order of tens of seconds. Thus, the PSM algorithm has higher computational efficiency and is favorable for the real-time imaging.



(a) BP algorithm (b) PSM algorithm

Figure 5. Imaging Time vs. Sampling Interval

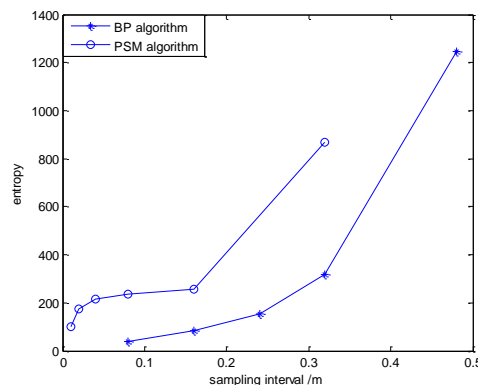


Figure 6. Imaging Entropy vs. Sampling Interval

Figure 6 demonstrates the relationship between the entropy of the image and the sampling interval for the BP and PSM algorithms. The image entropy for both algorithms increases with the sampling interval. For the same sampling interval, the entropy of the image produced by the BP algorithm is less than that produced by the PSM algorithm. So, the BP algorithm produces higher-quality images.

These results were obtained for a noise-free condition. In reality, the image quality will be affected by noise. Thus, we also simulated a noisy environment. Specifically, the scattered signal was corrupted with an additive Gaussian noise with zero mean and a fixed variance based on the desired signal-to-noise ratio (SNR). The entropy as a function of the SNR is shown in Figure 7. To make the entropy approximately equal, the sampling interval for the BP algorithm was 0.08 m and the sampling interval for the PSM algorithm was 0.01 m.

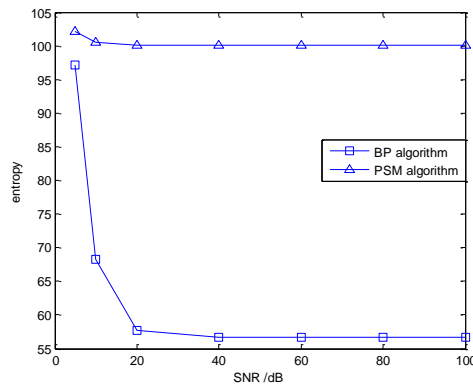


Figure 7. Entropy vs. SNR

From Figure 7, it can be observed that the PSM algorithm was largely unaffected by noise, and the added noise had a very small effect on the BP algorithm when the SNR was greater than 20 dB. Thus, the PSM algorithm is more robust than the BP algorithm.

4. Conclusion

UWB radar imaging of multiple targets through multi-layer walls was simulated, and results obtained using the BP algorithm and the PSM algorithm were compared. For both algorithms, the processing time and the image entropy depend on the sampling interval. The simulated results showed that the BP algorithm and the PSM algorithm can locate the targets precisely, but the image quality and the azimuthal resolution of the BP algorithm were better than those of the PSM algorithm. The processing time for the BP algorithm is significantly affected by the number of layers in the wall because accurate refraction points must be determined for every interface. The processing time for the PSM algorithm was on the order of tens seconds and the number of layers in the wall had only a minor effect, so the PSM algorithm is suitable for the real-time imaging. In the presence of noise, the PSM algorithm was robust, and the performance of the BP algorithm was slightly worse. The two algorithms have their respective advantages, so the choice of one or the other may be made based on practical requirements.

Acknowledgements

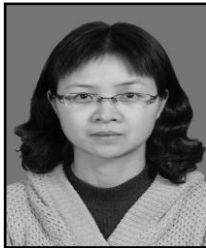
This work is supported by the National Natural Science Foundation of China (Grant No. 61071022, 61372045), the scientific research foundation of Nanjing University of Posts and Telecommunications(Grant No. NY215165), and University Science Research Project of Jiangsu Province(Grant No. TJ213012).

References

- [1] M. Dehmollaian and K. Sarabandi, "Refocusing through building walls using synthetic aperture radar", *IEEE Transactions on Geoscience and Remote Sensing*, vol. 46, no. 6, (2008), pp. 1589-1599.
- [2] F. F. Wang and Y. R. Zhang, "An electromagnetic inverse scattering approach based on support vector machine", *Acta Physica Sinica*, vol. 61, no. 8, (2012), pp. 084101-084108.(in Chinese)
- [3] J. G. Liu, L. J. Kong, X. B. Yang and Y. Jia, "Image auto-focusing with multi-layer nonhomogeneous wall in through-wall-radar imaging", *Radar Conferenc*, (2012), May 7-11, Atlanta, the USA, pp. 0543-0546.
- [4] F. Ahmad, M. G. Amin and S. A. Kassam, "Synthetic aperture beamformer for imaging through a dielectric wall", *IEEE Transactions on Aerospace and Electronic Systems*, vol. 41, no. 1, (2005), pp. 271-283.

- [5] F. Ahmad, Y. M. Zhang and M. G. Amin, "Three-dimensional wideband beamforming for imaging through a single wall", *IEEE Geoscience and Remote Sensing Letters*, vol. 5, no. 2, (2008), pp. 176-179.
- [6] G. Y. Wang and M. G. Amin, "Imaging through unknown walls using different standoff distances", *IEEE Transactions on Signal Processing*, vol. 54, no. 10, (2006), pp. 4015-4025.
- [7] S. Raffaele, D. N. Rosario, S. Francesco and P. Rocco, "TWI for an unknown symmetric lossless wall", *IEEE Transactions on Geoscience and Remote Sensing*, vol. 49, no. 8, (2011), pp. 2876-2886.
- [8] F. Ahmad, M. G. Amin and S. A. Kassam, "Synthetic aperture beamformer for imaging through a dielectric wall", *IEEE Transactions on Aerospace and Electronic Systems*, vol. 41, no. 1, (2005), pp. 271-283.
- [9] J. Gazdag, "wave equation migration with the phase-shift method", *Geophysics*, vol. 43, no. 7, (1978), pp. 1342-1351.
- [10] M. H. Skjeltvareid, T. Olofsson, Y. Birkelund and Y. Larsen, "Synthetic Aperture Focusing of Ultrasonic data from multilayered media using an omega-K algorithm", *IEEE transactions on ultrasonics, ferroelectrics, and frequency control*, vol. 58, no. 5, (2011), pp.1037-1048.
- [11] T. Olofsson, "Phase shift migration for imaging layered objects and objects immersed in water", *IEEE Transactions on Ultrasonics, Ferroelectrics, and Frequency Control*, vol. 57, no. 11, (2010), pp. 2522-2530.
- [12] X. Gu and Y. H. Zhang, "Autofocus imaging simulation for through-wall radar by using FDTD with unknown wall characteristics", *Proceeding of Asia-Pacific Microwave Conference*, (2010), pp. 1657-1660.

Authors



Huamei Zhang, she is lecturer at Nanjing University of Posts and Telecommunications now. She obtained her bachelor's degree in Nanjing University of Information Science & Technology and master's degree in Nanjing University of Posts and Telecommunications. Her major researches are numerical calculation of electromagnetic field, inverse scattering and imaging, *etc.*

Yerong Zhang, he is professor at Nanjing University of Posts and Telecommunications now. He obtained his Ph.D. in University of Electronic Science and Technology of China. His major researches are wireless communication, network optimization, electromagnetic scattering and inverse scattering, *etc.*

Fangfang Wang, she is lecturer at Nanjing University of Posts and Telecommunications now. She obtained her Ph.D. in Nanjing University of Posts and Telecommunications. Her major researches are numerical calculation of electromagnetic field, inverse scattering and imaging, *etc.*